

# An NADH-Dependent Bacterial Thioredoxin Reductase-like Protein in Conjunction with a Glutaredoxin Homologue Form a Unique Peroxiredoxin (AhpC) Reducing System in *Clostridium pasteurianum*<sup>†</sup>

C. Michael Reynolds,<sup>‡</sup> Jacques Meyer,<sup>§</sup> and Leslie B. Poole<sup>\*,‡</sup>

Department of Biochemistry, Wake Forest University School of Medicine, Winston-Salem, North Carolina 27157, and DBMS-BECP, CEA-Grenoble, 38054 Grenoble, France

Received September 17, 2001; Revised Manuscript Received November 19, 2001

**ABSTRACT:** Many eubacterial genomes including those of *Salmonella typhimurium*, *Streptococcus mutans*, and *Thermus aquaticus* encode a dedicated flavoprotein reductase (AhpF, Nox1, or PrxR) just downstream of the structural gene for their peroxiredoxin (Prx, AhpC) homologue to reduce the latter protein during turnover. In contrast, the obligate anaerobe *Clostridium pasteurianum* codes for a two-component reducing system upstream of the *ahpC* homologue. These three structural genes, herein designated *cp34*, *cp9*, and *cp20*, were previously identified upstream of the rubredoxin gene in *C. pasteurianum*, but were not linked to expression of the latter gene [Mathieu, I., and Meyer, J. (1993) *FEMS Microbiol. Lett.* 112, 223–227]. *cp34*, *cp9*, and *cp20* have been expressed in *Escherichia coli*, and their products have been purified and characterized. Cp34 and Cp9 together catalyze the NADH-dependent reduction of Cp20 to effect the reduction of various hydroperoxide substrates. Cp34, containing noncovalently bound FAD and a redox-active disulfide center, is an unusual member of the low-*M<sub>r</sub>* thioredoxin reductase (TrxR) family. Like *Escherichia coli* TrxR, Cp34 lacks the 200-residue N-terminal AhpC-reducing domain present in *S. typhimurium* AhpF. Although Cp34 is more similar to TrxR than to AhpF in sequence comparisons of the nucleotide-binding domains, experiments demonstrated that NADH was the preferred reductant (*K<sub>m</sub>* = 2.65 μM). Cp9 (a distant relative of bacterial glutaredoxins) is a direct electron acceptor for Cp34, possesses a redox-active CXXC active site, and mediates the transfer of electrons from Cp34 to several disulfide-containing substrates including 5,5'-dithiobis(2-nitrobenzoic acid), insulin, and Cp20. These three proteins are proposed to play a vital role in the defense of *C. pasteurianum* against oxidative damage and may help compensate for the putative lack of catalase activity in this organism.

Many obligate anaerobic bacteria are limited in their ability to tolerate reactive oxygen species (ROS)<sup>1</sup> due to the absence of catalase and/or superoxide dismutase (SOD) (1). Instead,

some anaerobic bacteria have been reported to express superoxide reductase (SOR), an enzyme that does not produce O<sub>2</sub> as a byproduct (unlike SOD or catalase) and may provide a selective advantage to anaerobes (1, 2). Unlike SOD, SOR produces hydrogen peroxide (H<sub>2</sub>O<sub>2</sub>) exclusively (reaction 1). In these organisms, H<sub>2</sub>O<sub>2</sub> must also be eliminated in order to avoid its cytotoxicity and deter the production of other highly toxic reactive oxygen species, such as hydroxyl radical (•OH). Peroxiredoxins (Prxs), in conjunction with a Prx reductase protein or system, may play an essential role in these anaerobic organisms by catalyzing the removal of H<sub>2</sub>O<sub>2</sub> as well as other hydroperoxide-containing species (reaction 2).

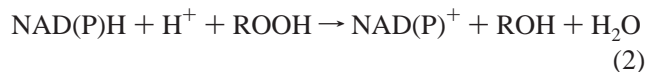
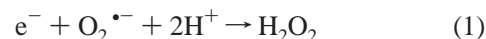
<sup>†</sup> This research was supported by National Institutes of Health Grant RO1 GM-50389 to L.B.P.

<sup>\*</sup> To whom correspondence should be addressed at the Department of Biochemistry, Wake Forest University School of Medicine, Medical Center Blvd., Winston-Salem, NC 27157. Tel: 336-716-6711; Fax: 336-716-7671; E-mail: lbpoole@wfubmc.edu; URL: <http://www.wfubmc.edu/biochem/faculty/Poole/poole.html>.

<sup>‡</sup> Wake Forest University School of Medicine.

<sup>§</sup> DBMS-BECP.

<sup>1</sup> Abbreviations: ROS, reactive oxygen species; SOD, superoxide dismutase; SOR, superoxide reductase; Trx, thioredoxin; TrxR, thioredoxin reductase; SDS, sodium dodecyl sulfate; SDS-PAGE, sodium dodecyl sulfate-polyacrylamide gel electrophoresis; IPTG, isopropyl β-D-thiogalactopyranoside; Fd, ferredoxin; *rub*, structural gene encoding rubredoxin; DTNB, 5,5'-dithiobis(2-nitrobenzoate); TNB, 2-nitro-5-thiobenzoate; LB, Luria-Bertani medium; Prx(s), peroxiredoxin(s); DTT, dithiothreitol; Grx(s), glutaredoxin(s); ESI-MS, electrospray ionization-mass spectrometry; GuHCl, guanidine hydrochloride; O<sub>2</sub><sup>•-</sup>, superoxide anion; H<sub>2</sub>O<sub>2</sub>, hydrogen peroxide; •OH, hydroxyl radical; Fd-TrxR, ferredoxin-dependent thioredoxin reductase; PFO, pyruvate-ferredoxin oxidoreductase; GAR, glutathione amide reductase; X-gal, 5-bromo-4-chloro-3-indolyl-β-D-galactopyranoside; AcPyAD(P)<sup>+</sup>, oxidized 3-acetylpyridine adenine dinucleotide (phosphate); AcPyAD(P)H, reduced 3-acetylpyridine adenine dinucleotide (phosphate); Buffer A, 25 mM potassium phosphate at pH 7.0, with 1 mM EDTA; Buffer B, 5 mM potassium phosphate at pH 6.5, with 1 mM EDTA.



Prxs are ubiquitous proteins (3); studies of Prxs from *Salmonella typhimurium* (4–6), *Helicobacter pylori* (7), and *Crithidia fasciculata* (8) have revealed that they possess the ability to metabolize various peroxide substrates including H<sub>2</sub>O<sub>2</sub>, organic hydroperoxides, and lipid hydroperoxides. Several different types of Prx reductase systems have been

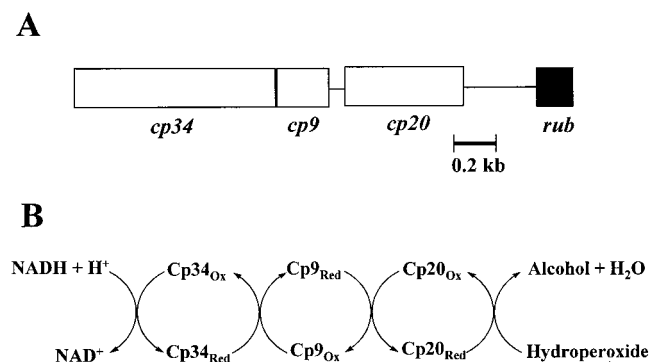


FIGURE 1: Genetic organization and electron-transfer pathways of the alkyl hydroperoxide reductase system from *C. pasteurianum*. The three open reading frames of the system are upstream of *rub* (rubredoxin) in the *C. pasteurianum* genome as shown in panel A. The first open reading frame, *cp34* (924 bp), encodes a bacterial TrxR family member. The second open reading frame, *cp9* (225 bp), encodes a distant homologue of bacterial glutaredoxins while the third open reading frame, *cp20* (534 bp), codes for a member of the 2-Cys Prx family. As depicted in panel B, the three proteins form an alkyl hydroperoxide reductase system capable of metabolizing various hydroperoxide substrates by utilizing reducing equivalents from NADH. The NADH-reduced flavoprotein, Cp34, reduces the glutaredoxin-like Cp9 which in turn reduces the Prx component, Cp20. The reduced form of Cp20 then catalyzes the conversion of the hydroperoxide substrate to alcohol and water.

identified. AhpC, the Prx from *S. typhimurium*, is reduced by AhpF, an FAD-containing pyridine nucleotide:disulfide oxidoreductase (4, 6). AhpF is a highly efficient and specific reactivator of AhpC present in most eubacteria (9). In cases where AhpF is not expressed but an alternative Prx-activation system has been identified, at least two or more redox components are involved in the reactivation process. For example, *H. pylori* and *Saccharomyces cerevisiae* utilize thioredoxin reductase (TrxR) and thioredoxin (Trx) to reduce their respective Prxs (7, 10). Another reactivation system for a Prx homologue has been found in *Crithidia fasciculata*; NADPH, trypanothione reductase, trypanothione, and trypanredoxin form a unique cascade of reducing power that facilitates the reduction of that organism's Prx (trypanredoxin peroxidase) (8).

*Clostridium pasteurianum*, an obligate anaerobe responsible for a significant amount of the nitrogen fixation that occurs in soil (11), has previously been reported to encode a Prx homologue (12). The latter gene (designated *cp20* in this report) is the last open reading frame of an operon including two other open reading frames (designated *cp34* and *cp9*) and is located upstream of the rubredoxin-encoding gene (Figure 1, panel A) (12). The gene product of *cp34* is homologous with low- $M_r$  TrxRs (37% identity to *Escherichia coli* TrxR); Cp9 is distantly related to bacterial glutaredoxins (Grxs) (31% identity to *E. coli* Grx1). Interestingly, Cp20, with 35% identity to *S. typhimurium* AhpC, is more closely related to some 2-Cys Prxs from mammalian sources (58% identity to *Homo sapiens* PrxII) than to those of most other eubacteria (7).

We report herein that Cp34, Cp9, and Cp20 comprise a unique three-component alkyl hydroperoxide reductase system that catalyzes the NADH-dependent reduction of both  $H_2O_2$  and organic hydroperoxides (Figure 1, panel B). This enzyme system from *C. pasteurianum* is the first example of an alkyl hydroperoxide reductase system that utilizes a

Grx-like protein, Cp9, to directly mediate electron transfer from the flavoprotein component, Cp34, to the Prx.

## EXPERIMENTAL PROCEDURES

**Materials.** Bacteriological media components were from Difco Laboratories (Detroit, MI). Vent DNA polymerase and some restriction enzymes were from New England Biolabs (Beverly, MA). Other restriction enzymes and T4 DNA ligase were from Promega (Madison, WI). Cumene hydroperoxide, tricine, streptomycin sulfate, protocatechuic acid, protocatechuic 3,4-dioxygenase, spinach ferredoxin (Fd)-NADP<sup>+</sup> reductase, FAD, FMN, ampicillin, *Naja naja* venom phosphodiesterase, oxidized 3-acetylpyridine adenine dinucleotide (AcPyAD<sup>+</sup>), oxidized 3-acetylpyridine adenine dinucleotide phosphate (AcPyADP<sup>+</sup>), and bovine pancreas insulin were from Sigma (St. Louis, MO). NADPH and NADH were from Boehringer Mannheim (Mannheim, Germany). Acrylamide/Bis solution (29:1) was purchased from Bio-Rad (Hercules, CA). Gelcode blue stain reagent was from Pierce (Rockford, IL). Isopropyl- $\beta$ -D-thiogalactopyranoside (IPTG) and 5-bromo-4-chloro-3-indolyl- $\beta$ -D-galactopyranoside (X-Gal) were from Inalco (Milan, Italy). Sodium dodecyl sulfate (SDS), glycerol, ultrapure glycine, ultrapure urea, EDTA, dithiothreitol (DTT), 5,5'-dithiobis(2-nitrobenzoic acid) (DTNB), and other reagents were purchased from Research Organics (Cleveland, OH). HPLC-grade acetonitrile, sodium hydrosulfite, agarose medium EEO (electrophoresis grade), and  $H_2O_2$  were from Fisher (Fairlawn, NJ). Ethyl hydroperoxide was from Polysciences, Inc. (Warrington, PA). Buffer A (25 mM potassium phosphate at pH 7.0, with 1 mM EDTA) was used unless otherwise indicated.

**Sequence Analysis.** The BestFit program of SeqWeb (Web-based Sequence Analysis v. 1.2) in conjunction with the University of Wisconsin Genetics Computer Group (GCG) package (v. 10.1) was used to perform pairwise comparisons. Cp34, Cp9, and Cp20 homologues were identified through TBLASTN (13) searches with the sequence of each of the proteins. The multiple sequence alignment of Cp34, TrxR, and AhpF was generated using CLUSTAL W available at the Biology Workbench (v. 3.2) of the San Diego Supercomputer Center (<http://workbench.sdsc.edu/>) (14).

**Subcloning and Expression of *cp34*, *cp9*, and *cp20*.** pCPRD1 (12), a pUC18-derived plasmid containing a 3.9 kb *Bgl*III–*Hind*III insert of *C. pasteurianum* genomic DNA cloned into the vector's *Bam*HI and *Hind*III sites, served as the template in PCR reactions to amplify the three genes of interest. Each coding sequence was amplified using PCR primers synthesized in the DNA Synthesis Core Laboratory of the Comprehensive Cancer Center of Wake Forest University. The sequences of the synthesized primers were as follows: (Cp34) forward 5'-GGCAAGCTTAGGAGG-AAGTATAGATGAAAGAAGAGAAGC-3' and reverse 5'-CCGGATCCGATATGTTGGTGTGGAAT-3'; (Cp9) forward 5'-GGCAAGCTTAGGAGGAAGTATAGATGATT-AAAATAT-3' and reverse 5'-CCGGATCCAAAAGTAGTC-TATTTTC-3'; (Cp20) forward 5'-GGCAAGCTTAGGAG-GAAGTATAGATGGAGAGATTAGTGGG-3' and reverse 5'-CCGGATCCTTATAAGTTGTCATC-3' (engineered *Bam*HI and *Hind*III restriction sites are in boldface type, ribosome-binding sites are underlined, and the ATG start codons are in italics). PCR mixtures (50  $\mu$ L) contained 200

$\mu\text{M}$  deoxynucleoside triphosphates, 2 units of Vent DNA polymerase, 20 pmol each of the forward and reverse primers, 1 mM  $\text{MgCl}_2$ , and 0.1  $\mu\text{g}$  of template DNA. Reactions were carried out in a Mini Cyclor (MJ Research, Waltham, MA) using similar PCR conditions for all three: 95 °C for 30 s–2 min, 45 or 55 °C for 45 s–1 min, and 72 °C for 1–1.5 min (30–35 cycles). The PCR products for *cp34* and *cp9* were purified using the QIAquick PCR cleanup kit (Qiagen, Studio City, CA) and were ligated into the pCR2.1 TA cloning vector (Invitrogen, Carlsbad, CA). Although primers were designed to introduce a *Hind*III site upstream and a *Bam*HI site downstream of the three genes in order to facilitate subcloning of each gene into pOXO4 (15), *cp34* and *cp9* were subcloned instead (for optimal expression) into pTrc99A (Amersham Pharmacia Biotech Inc., Piscataway, NJ) using the *Bam*HI site and an *Eco*RI site from the multiple cloning site of pCR2.1. Fragments containing *cp34* or *cp9* were purified from 0.8% agarose gels using the Gene Clean II Kit (Bio 101, Inc., Vista, CA) and then subcloned into the corresponding sites of pTrc99A. Subcloning of *cp20* was achieved by a *Hind*III–*Bam*HI digest of the appropriately sized PCR product and subsequent ligation into the corresponding sites of pOXO4.

Ligated DNA was transformed into competent *E. coli* XL-1 Blue cells (Stratagene, La Jolla, CA) for pTrc99A/*cp34* and pTrc99A/*cp9*, or into JM109(DE3) cells (Promega) for pOXO4/*cp20*. Single colonies were selected on Luria–Bertani (LB) plates containing ampicillin at 50  $\mu\text{g}/\text{mL}$  for the pTrc99A-derived constructs and plates containing 25  $\mu\text{g}/\text{mL}$  chloramphenicol for the pOXO4-derived construct, and extracts from small-scale cultures were evaluated for gene expression on SDS–polyacrylamide gels after induction with 0.4 mM IPTG. Due to the low  $M_r$  of Cp9, it was necessary to employ Tris–tricine-buffered SDS–polyacrylamide gels (16) to examine Cp9-overexpressing clones. The coding regions for all three genes were sequenced in their entirety by the DNA sequence analysis core laboratory of the Comprehensive Cancer of Wake Forest University. Procedures for culturing and storing plasmid-harboring bacteria were essentially the same as those reported earlier (6,7).

**Purification of Recombinant Cp34.** Cultures of *E. coli* XL-1 Blue cells harboring pTrc99A/*cp34* plasmid were grown in 10 L of ampicillin-containing LB medium supplemented with 0.2% glucose in a New Brunswick BioFlo 2000 fermentor (New Brunswick Scientific, Edison, NJ) after inoculation to 2% from an overnight culture. IPTG at 0.4 mM (final concentration) was added at  $A_{600} = 2.0$  (approximately mid-log phase in the fermentor growth), and the growth was continued overnight. Harvested cell pellets were stored at –20 °C until needed. Extracts from mechanically disrupted cells were treated with streptomycin sulfate to remove nucleic acids. A Cp34-enriched pellet obtained by ammonium sulfate fractionation (30–75% saturation in Buffer A) (6) was resuspended and dialyzed against Buffer A overnight. The dialyzed extract was then applied to a Q Sepharose Fast Flow FPLC column preequilibrated with 80 mM potassium phosphate buffer (pH 7.0, including 1 mM EDTA). The column was washed with this buffer and then eluted with a linear gradient of potassium phosphate buffer from 80 to 160 mM. Fractions containing the protein of interest were analyzed by SDS–polyacrylamide gel electrophoresis (SDS–PAGE) and by  $A_{280}/A_{450}$  ratios, and then

pooled and brought to 30% saturation in ammonium sulfate. The pool was then loaded onto a Phenyl Sepharose 6 Fast Flow column preequilibrated with Buffer A containing 30% saturated ammonium sulfate. The column was washed and then eluted with a linear gradient of Buffer A containing 30–0% ammonium sulfate. Again, fractions were analyzed for Cp34 by SDS–PAGE, and pure fractions were pooled, dialyzed against Buffer A, and stored at –20 °C until further use.

**Purification of Recombinant Cp9.** A 10 L culture of *E. coli* XL-1 Blue harboring the pTrc99A/*cp9* expression plasmid was grown in the fermentor and induced as described above for Cp34 expression. Production of the crude extract and streptomycin sulfate treatment were as described above with the exception that 5 mM potassium phosphate, pH 6.5, with 1 mM EDTA (Buffer B) was used for all steps instead of Buffer A. Ammonium sulfate fractionation (20–80% saturation in Buffer B) yielded a Cp9-enriched fraction that was resuspended in Buffer B and dialyzed overnight before being loaded onto a Whatman CM52 cation-exchange column preequilibrated in the same buffer. The column was washed with Buffer B and then eluted with a linear gradient from 5 to 30 mM potassium phosphate. Fractions were analyzed on 12% polyacrylamide (Tris–tricine) gels, and pure fractions were pooled and dialyzed against Buffer A prior to concentration and subsequent storage at –20 °C.

**Purification of Recombinant Cp20.** Cultures of *E. coli* JM109(DE3) cells harboring the pOXO4/*cp20* plasmid were grown in 10 L of chloramphenicol-containing LB medium, induced with IPTG for 3 h, harvested, and stored as described above. Similarly prepared crude extracts were treated with streptomycin sulfate, subjected to 20% and 70% saturation ammonium sulfate cuts, and dialyzed as for Cp34. The protein was further purified on Q Sepharose and Phenyl Sepharose columns as described for Cp34 except that the gradients used were 50–200 mM potassium phosphate and 20–0% saturated ammonium sulfate, respectively. Fractions containing pure Cp20 were pooled, dialyzed against Buffer A, and concentrated prior to storage at –20 °C.

**Other Protein Purifications.** *S. typhimurium* AhpF, *E. coli* TrxR, and *E. coli* Trx were expressed and purified as previously described (6, 17, 18). *C. pasteurianum* rubredoxin was purified as reported previously (12).

**Molecular Weight Determination of Cp34, Cp9, and Cp20 by Mass Spectrometry.** Electrospray ionization-mass spectrometry (ESI-MS) determinations were made on a VG Quattro II triple quadrupole mass spectrometer from Micro-mass (Whytenshaw, U.K.) in the GC-Mass Spectrometry Laboratory of the Comprehensive Cancer Center of Wake Forest University. Each protein was washed extensively with distilled water to remove salts in ultrafiltration units [a Centricon CM-50 for Cp34 and Orbital Biosciences (Topsfield, MA) Apollo concentrators (5 kDa cutoff) for Cp9 and Cp20]. A 10  $\mu\text{M}$  solution of each protein in 50% HPLC-grade acetonitrile and 1% formic acid was then injected by nanoflow into the mass spectrometer in the positive ion mode.

**Identification of the Flavin Cofactor of Cp34 by Mass Spectrometry.** The flavin cofactor of Cp34 was released from the protein and analyzed as described previously (19). Cp34 was washed extensively with distilled water in a Centricon CM-50 ultrafiltration unit to remove salts. Next, the protein

solution was boiled for 30 min and then centrifuged for 25 min at 14 000 rpm to pellet the denatured protein. The resulting supernatant was then passed through an Apollo concentrator (5 kDa cutoff) to remove any protein that had not been removed during the centrifugation step. A solution of 50% HPLC-grade acetonitrile and 1% formic acid containing approximately 10  $\mu\text{M}$  of the released flavin was then analyzed by ESI-MS in the negative ion mode. A solution containing 10  $\mu\text{M}$  each of FAD and FMN in 50% acetonitrile and 1% formic acid was used to optimize parameters for ESI-MS analysis of the cofactor.

**Analytical Ultracentrifugation Experiments.** Sedimentation equilibrium analyses were performed essentially as described previously (17). All oxidized proteins were washed in Apollo concentrators prior to ultracentrifugation to reconstitute the proteins in Buffer A containing 150 mM NaCl. Solutions of reduced Cp9 and reduced Cp20 were made by preincubation (4 °C overnight) of the proteins with a 20-fold excess of DTT. Proteins were then washed free of DTT in Apollo concentrators and reconstituted in Buffer A containing 150 mM NaCl. Three concentrations each (115  $\mu\text{L}$  per sample) of Cp34 (3–85  $\mu\text{M}$ ), oxidized and reduced Cp9 (12–104  $\mu\text{M}$ ), and oxidized and reduced Cp20 (6–50  $\mu\text{M}$ ) were loaded into six-sectored Epon charcoal centerpieces from Beckman Instruments Inc. (Palo Alto, CA) along with 125  $\mu\text{L}$  of the buffers from the final filtrate as reference. Samples were brought to three rotor speeds each of 10 000–18 000 rpm for Cp34, 21 000–36 000 rpm for Cp9, and 5500–12 000 rpm for Cp20 and allowed to equilibrate at 20 °C for 12, 14, and 16 h in a Beckman Optima XL-A analytical ultracentrifuge. The cells were then scanned, and absorbance data were collected at 280 nm for all protein samples (data were also collected at 450 nm for the Cp34 sample). Global analysis of 8–12 different data sets for each protein sample was performed using the Windows version of NONLIN (20). No data at or above 1.4 absorbance units were used in the analyses. Values of 0.7486, 0.7472, and 0.7392  $\text{cm}^3 \text{g}^{-1}$  for the partial specific volumes of Cp34, Cp9, and Cp20, respectively, were calculated from the amino acid compositions (21). The solvent density, at 1.0077  $\text{g cm}^{-3}$ , was measured using a DA-310M precision density meter (Mettler Toledo, Highstown, NJ) thermostated at 20 °C.

**Spectroscopic Experiments.** A thermostated Milton Roy Spectronic 3000 diode array spectrophotometer with 0.35 nm resolution was used to collect all absorbance spectra and to carry out enzymatic assays and anaerobic titration experiments. Assays were also done using an Applied Photophysics DX.17MV stopped-flow spectrofluorometer thermostated at 25 °C. Fluorescence spectra were recorded using an SLM Aminco Bowman Series 2 luminescence spectrophotometer from Thermo Spectronic (Rochester, NY). Anaerobic cuvette assemblies and the preparation of anaerobic dithionite and NADH solutions were described previously (5, 18). All anaerobic experiments included an oxygen-scrubbing system consisting of protocatechuic acid and protocatechuate 3,4-dioxygenase. Methyl viologen was added at a molar ratio of 1:100 relative to Cp34 to promote equilibration between redox centers during dithionite titrations.

Methods for determining extinction coefficients of proteins at 280 nm using microbiuret assays and for determining the extinction coefficient of Cp34's bound flavin were described

previously (6). The experimentally obtained extinction coefficients at 280 nm for Cp9 and Cp20 were  $12\,500 \pm 100$  and  $25\,900 \pm 200 \text{ M}^{-1} \text{ cm}^{-1}$ , respectively. The extinction coefficient of Cp34 at 450 nm was  $12\,700 \pm 100 \text{ M}^{-1} \text{ cm}^{-1}$ . To determine the concentrations of other proteins, the following extinction coefficients were used: *E. coli* TrxR,  $11\,300 \text{ M}^{-1} \text{ cm}^{-1}$  (454 nm) (22); *E. coli* Trx,  $13\,700 \text{ M}^{-1} \text{ cm}^{-1}$  (280 nm) (23); *S. typhimurium* AhpF,  $13\,100 \text{ M}^{-1} \text{ cm}^{-1}$  (450 nm) (6); *C. pasteurianum* rubredoxin,  $6600 \text{ M}^{-1} \text{ cm}^{-1}$  (490 nm) (24); and spinach Fd-NADP<sup>+</sup> reductase,  $85\,000 \text{ M}^{-1} \text{ cm}^{-1}$  (275 nm) (25). Extinction coefficients for all reduced and oxidized pyridine nucleotides, free FAD, and TNB were those previously reported (6). An extinction coefficient of  $12\,200 \text{ M}^{-1} \text{ cm}^{-1}$  was used for free FMN (26).

Assays for the free thiol groups of Cp34, Cp9, and Cp20 were carried out by incubation of oxidized protein solutions in the presence and absence of guanidine hydrochloride (GuHCl) at a final concentration of 4 M, followed by addition of 100  $\mu\text{M}$  DTNB. Reduced proteins were prepared in three different ways for thiol determinations. Cp34 was preincubated anaerobically with excess NADH prior to denaturation and DTNB assay. Cp9 was incubated with a catalytic amount of Cp34 (1/200th mol equiv) and excess NADH (5-fold) under anaerobic conditions prior to addition of GuHCl and DTNB. Cp9 and Cp20 were preincubated with a 20-fold excess of DTT, washed free of DTT using a Centricon CM-10 ultrafiltration unit for Cp20 and an Apollo concentrator (5-kDa cutoff) for Cp9, and assayed for free thiols in the presence and absence of 4 M GuHCl.

**Steady-State Kinetic Analysis of Cp34 Using DTNB- and Insulin-Linked Assays.**  $K_m$  and  $k_{cat}$  measurements of Cp34 with its two substrates, NADH and Cp9, were carried out using a DTNB-linked assay essentially as described previously (6, 27). Briefly, assays contained 50 mM Tris-HCl at pH 8.0, 0.5 mM EDTA, 100 mM ammonium sulfate, 500  $\mu\text{M}$  DTNB, 0.8–20  $\mu\text{M}$  NADH, 0–15  $\mu\text{M}$  Cp9, and 20 nM Cp34. The increase in  $A_{412}$  due to the production of TNB was measured using the stopped-flow spectrophotometer. One stopped-flow syringe contained a fixed concentration of NADH while the other syringe contained the DTNB, Cp34, and varying concentrations of Cp9. The rate data were transformed and displayed in primary Hanes–Woolf plots (28). Slopes obtained for each concentration of Cp9 or NADH from primary Hanes plots were replotted in secondary Hanes–Woolf plots (slope replots) to obtain the true  $k_{cat}$  and the true  $K_m$  values.

The ability of Cp34 to reduce *E. coli* Trx or for *E. coli* TrxR to reduce Cp9 was assessed using the DTNB-linked assay as well. Reaction mixtures at 25 °C contained the same buffer, but 150  $\mu\text{M}$  NADH (Cp34) or NADPH (TrxR), 0–30  $\mu\text{M}$  Trx or Cp9, and 50 nM of the respective heterologous reductase, Cp34 or TrxR.

Assays using bovine pancreas insulin as the electron acceptor for Cp9 were carried out following the method of Holmgren (29), and included 150  $\mu\text{M}$  NADH, 100  $\mu\text{M}$  bovine pancreas insulin, 50 mM potassium phosphate at pH 7.0, and 1 mM EDTA, 0.25–20  $\mu\text{M}$  Cp9, and 20 nM Cp34 in a total volume of 0.5 mL at 25 °C. Absorbance changes were monitored at 340 nm.  $k_{cat}(\text{app})$  and  $K_m(\text{app})$  values were determined using the ENZFITTER program (30). The insulin-linked assay was also used to assess AhpF's ability to reduce Cp9. AhpF at 0.5  $\mu\text{M}$  was assayed with 10 and 20

$\mu\text{M}$  Cp9 (a complete set of steady-state assays was not done with AhpF due to its lack of activity with Cp9).

**Other Spectrophotometric Assays.** The oxidase activities of AhpF, TrxR, and Cp34 were determined as described previously (6). Assays were conducted at 25 °C in 1 mL of air-saturated buffer containing 150  $\mu\text{M}$  NADH (NADPH for TrxR), and 50 mM potassium phosphate at pH 7.5, 0.5 mM EDTA. The amounts of Cp34 or AhpF ranged from 30 to 90 nM while the amount of TrxR ranged from 0.5 to 1  $\mu\text{M}$ .

Transhydrogenase activity assays with Cp34, AhpF, and TrxR were also done as described previously (6). Assays were conducted at 25 °C in 1 mL of buffer containing 150  $\mu\text{M}$  each of NADH (NADPH for TrxR) and AcPyAD<sup>+</sup> (AcPyADP<sup>+</sup> for TrxR), and the same ammonium sulfate-containing buffer as used for the DTNB-linked assays. AhpF amounts ranged from 3 to 9 nM, TrxR from 5 to 20 nM, and Cp34 from 90 to 150 nM. Assays were monitored at 390 nm, a wavelength at which the production of AcPyAD(P)H can be assessed.

Peroxidase assays were carried out on the stopped-flow spectrofluorometer at 25 °C with 0.5  $\mu\text{M}$  Cp34, 10  $\mu\text{M}$  Cp9, and 10  $\mu\text{M}$  Cp20. Cp9 and/or Cp20 were omitted in some assays. Reactions contained 150  $\mu\text{M}$  NADH, 50 mM potassium phosphate at pH 7.0, 100 mM ammonium sulfate, and 1 mM of hydroperoxide substrate (cumene hydroperoxide, H<sub>2</sub>O<sub>2</sub>, or ethyl hydroperoxide). AhpF (0.5  $\mu\text{M}$ ) was also substituted for both Cp34 and Cp9 (in the presence of cumene hydroperoxide) in order to determine if Cp20 is a substrate for AhpF.

Rubredoxin reductase assays with the Cp34–Cp9 system employed a modification of previously described methods (31). Briefly, assay mixtures contained 150  $\mu\text{M}$  NAD(P)H, 152  $\mu\text{M}$  rubredoxin ( $A_{490} \sim 1.0$ ), and 100 mM Tris-HCl at pH 7.5 in a total volume of 1.0 mL. The decrease in  $A_{490}$  due to rubredoxin reduction was monitored after the addition of Cp34 (0.1–1  $\mu\text{M}$ ), in the presence and absence of Cp9 (10  $\mu\text{M}$ ), or of 20 nM spinach Fd-NADP<sup>+</sup> reductase (the positive control) to the assay mixture.

**Fluorometric Assay of Cp20 Reduction by DTT-Reduced Cp9.** Cp9 was treated with a 20-fold excess of DTT overnight at 4 °C and then washed free of the reagent in an Apollo concentrator (5 kDa cutoff). Thiol contents of Cp9 after the DTT treatment were  $2.26 \pm 0.04$ , indicative of complete reduction of the active site disulfide of Cp9. Fluorometric measurements of solutions of reduced and oxidized Cp9 made using an SLM Aminco Bowman Series 2 luminescence spectrophotometer revealed that reduced Cp9 ( $\lambda_{\text{max,ex}} = 280$  nm,  $\lambda_{\text{max,em}} = 346$  nm) exhibits a 2.2-fold greater tryptophan fluorescence than oxidized Cp9 at the same wavelength. This difference allowed us to directly measure the rate of electron transfer from reduced Cp9 to Cp20 on the stopped-flow spectrofluorometer (using a 320 nm filter). Assays in the peroxidase assay buffer included Cp9 at 5–35  $\mu\text{M}$ , and Cp20 and H<sub>2</sub>O<sub>2</sub> at 1  $\mu\text{M}$  and 1 mM, respectively. The fluorescence decrease was converted to the amount of Cp9 oxidized by normalization to the fluorescence difference between reduced and oxidized Cp9 using the following formula:  $\Delta\text{concentration}/\text{time} = 1. \Delta\text{fluorescence}/\text{time} \div \text{fluorescence}/\text{concentration}$ , where fluorescence/concentration = (2. fluorescence of reduced Cp9 + 3. fluorescence of oxidized Cp20 and H<sub>2</sub>O<sub>2</sub> - 4. fluorescence of the buffer - 5. fluorescence of oxidized Cp9, oxidized Cp20 and H<sub>2</sub>O<sub>2</sub>)  $\div$  concentration of

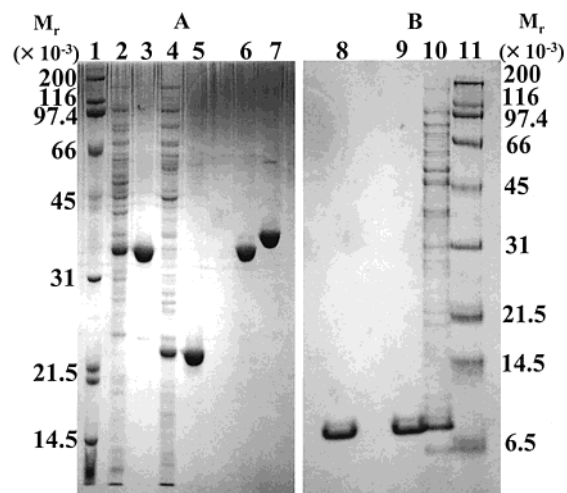


FIGURE 2: SDS-PAGE analysis of purified Cp34, Cp9, and Cp20. (A) Crude extracts and purified, recombinant Cp34 (lanes 2, 3, and 6) and Cp20 (lanes 4, 5, and 7) were analyzed in reducing (lanes 2–5) or nonreducing (lanes 6–7) sample buffer on the same 12% polyacrylamide gel as follows: lane 1, molecular mass markers (Broad Range Molecular Weight Standards from Bio-Rad, Hercules, CA); lane 2, 15  $\mu\text{g}$  of the crude extract from the Cp34 purification (as described under Experimental Procedures); lane 3, 6  $\mu\text{g}$  of pure Cp34; lane 4, 15  $\mu\text{g}$  of the crude extract from the Cp20 purification; lane 5, 6  $\mu\text{g}$  of pure Cp20; lane 6, 6  $\mu\text{g}$  of pure, nonreduced Cp34; lane 7, 6  $\mu\text{g}$  of pure, nonreduced Cp20. (B) Crude extracts and purified, recombinant Cp9 were analyzed on a 12% polyacrylamide (in Tris–tricine) gel as follows: lane 8, 6  $\mu\text{g}$  of pure Cp9 prepared in nonreducing sample buffer; lane 9, 6  $\mu\text{g}$  of pure Cp9 prepared in reducing sample buffer; lane 10, 15  $\mu\text{g}$  of the crude extract from the Cp9 purification; lane 11, molecular mass markers.

reduced Cp9; each number indicates a separate measurement on the stopped-flow spectrofluorometer.

**N-Terminal Sequencing of Previously Purified Ferredoxin-Dependent TrxR (Fd-TrxR) and Trx from *C. pasteurianum*.** To determine if Cp34 and Cp9 were the same proteins that had been previously characterized as an Fd-dependent TrxR–Trx system from *C. pasteurianum* (32, 33), both Fd-TrxR and Trx (obtained from Dr. Bob Buchanan) were subjected to Edman degradation for 20 cycles for amino acid sequence analysis by the Protein Analysis Core Laboratory of the Comprehensive Cancer of Wake Forest University.

## RESULTS AND DISCUSSION

**Molecular Weights and Oligomeric States of Cp34, Cp9, and Cp20.** Cp34, Cp9, and Cp20 were all expressed in *E. coli* and purified to homogeneity as judged by SDS-PAGE (Figure 2). All three enzymes were obtained as soluble proteins after induction with IPTG at 37 °C. Pure Cp34 migrated in SDS-polyacrylamide gels as an  $M_r$  33 000 protein under both reducing and nonreducing conditions (Figure 2, panel A), while Cp9 gave an apparent  $M_r$  of 8000 under both conditions (Figure 2, panel B). As shown in Table 1, the molecular weights of both Cp34 and Cp9 determined by ESI-MS were in agreement with the molecular weights predicted from the amino acid sequence of each protein. The  $M_w$  values of the native proteins obtained from sedimentation equilibrium studies revealed that Cp34 is a dimer like TrxR (34) and AhpF (17), while Cp9 is monomeric in both oxidized and reduced forms (Table 1).

Cp20 migrated with an apparent  $M_r$  of 22 000 on reducing SDS-PAGE but as a higher  $M_r$  species (39 000) when

Table 1: Sizes, Thiol Contents, and Cofactors of Cp34, Cp9, and Cp20

	Cp34	Cp9	Cp20
predicted subunit mass <sup>a</sup>	34215	8607	20036
mass by ESI-MS	34216.6 ± 2.5	8605.4 ± 0.2	40041.4 ± 1.4
<i>M<sub>w</sub></i> from sedimentation equilibrium			
oxidized	69500 ± 1700	9010 ± 240	42500 ± 900
reduced	NS <sup>b</sup>	9700 ± 200	NS
thiol contents			
oxidized, native	0.13 ± 0.02	0.10 ± 0.04	0.18 ± 0.05
oxidized, denatured	0.11 ± 0.01	0.12 ± 0.01	1.08 ± 0.01
reduced, native	NS	2.28 ± 0.02	2.11 ± 0.07
reduced, denatured	1.88 ± 0.03	2.26 ± 0.12	3.01 ± 0.05
cofactor	0.9 FAD/subunit	none	none

<sup>a</sup> Molecular weights were predicted using the ProtParam tool from <http://www.expasy.ch/tools/protparam.html>. <sup>b</sup> NS = not shown. Reduced Cp34 is not air-stable, and reduced Cp20 was analyzed, but was a heterogeneous mixture of species with an average *M<sub>w</sub>* larger than the dimer (as described in the text).

prepared in nonreducing sample buffer (Figure 2, panel A). The higher *M<sub>r</sub>* species indicated that Cp20 is in its oxidized form as purified and contains one or more intersubunit disulfide bonds. The covalent linkage between Cp20's two subunits is consistent with previous studies of other members of the 2-Cys Prx family; oxidized AhpC was previously shown to be a covalently linked dimer (35). ESI-MS analysis of oxidized Cp20 confirmed the dimeric molecular weight of the oxidized protein (Table 1). However, these data were not in complete agreement with the predicted molecular weight of a Cp20 dimer (a difference of 27 amu per dimer between expected and experimental values, if one takes into account the loss of 4 H<sup>+</sup> due to disulfide formation). Sequence analysis of the expression plasmid pOXO4/*cp20* revealed no inadvertent mutations in the coding sequence, suggesting that the discrepancy in the molecular weight of Cp20 was due to the misreading of a codon. Evidence for a codon misread came from ESI-MS data of DTT-reduced Cp20. Two different species, a species of 20 036 amu (the molecular weight predicted from the amino acid composition) and a species of 20 008 amu, were detected in the reduced Cp20 sample. These data were consistent with the value from mass analysis of the primary species in the oxidized protein sample, 40 041 amu, if this mass value represents a heterodimeric form of the two species found in the oxidized sample (smaller amounts of homodimeric forms of each of the two species were also present). As the gene for Cp20 has multiple low-usage codons, we hypothesized that one of these codons could have rendered a change in an amino acid at one position for some of the Cp20 subunits (e.g., a substitution of Lys for Arg at one of the four AGA codons or at one of the three AGG codons, giving rise to a decrease of 28 amu per subunit) (36, 37). A codon misread was confirmed when N-terminal sequence analysis of Cp20 revealed that the third amino acid, corresponding to an AGA codon, is a mixture of Arg (64%) and Lys (36%). Assay data presented below indicated a lack of effect of this substitution on the catalytic function of Cp20.

Results of sedimentation equilibrium studies of both oxidized and reduced Cp20 revealed that Cp20 is a dimer in its oxidized form, but exists as a heterogeneous mixture of species with an average *M<sub>w</sub>* larger than dimer in its reduced

form (Table 1). Crystallographic studies of four Cp20 homologues have revealed that other 2-Cys Prxs form dimers and/or decamers, as well (38–40) (Wood, Z. A., and Karplus, P. A., unpublished observations). A tentative conclusion from these structural studies, that oxidized 2-Cys Prx proteins tend to be dimeric (38) while reduced (39) or over-oxidized (reduced-like) 2-Cys Prxs (40) tend to be decameric, has been verified by recent studies with AhpC from *S. typhimurium* (Wood, Z. A., Poole, L. B., Hantgan, R. R., and Karplus, P. A., unpublished data). In the latter case, redox-dependent oligomerization was characterized by sedimentation equilibrium and velocity analyses, although in this case the reduced protein was completely in the decameric form while oxidized AhpC was a mixture including dimeric through decameric forms. Thus, the dimer–dimer interface of Cp20 is destabilized relative to that of *S. typhimurium* AhpC, although the relative destabilization of this interface on oxidation of the proteins to their disulfide-containing forms is a characteristic common to both proteins.

*Thiol Quantitations of Cp34, Cp9, and Cp20.* No thiols could be detected in oxidized Cp34 (native or denatured) or oxidized Cp9 (native or denatured) (Table 1). However, approximately two thiols could be detected following the reduction and then denaturation of both Cp34 and Cp9 (native, reduced Cp9 also exhibited two reactive thiols). These thiol titers were indicative of redox-active disulfide centers within each of these proteins. The predicted amino acid sequences of both Cp34 and Cp9 each contain one C-X-X-C motif (Cys136-Glu-Leu-Cys139 in Cp34 and Cys10-Pro-Trp-Cys13 in Cp9), and in each case, these putative redox centers aligned perfectly with those previously identified in homologous proteins (*E. coli* TrxR and Grx1).

No free thiols could be detected in oxidized, native Cp20 while the thiol titer determined for oxidized, denatured Cp20 yielded approximately one thiol per subunit (Table 1). Approximately two thiols were detected in reduced, native Cp20 while reduced, denatured Cp20 exhibited approximately three thiols. Cp20 therefore contains one nonreactive thiol that is buried in the native enzyme but accessible to DTNB in the denatured protein. Also, the high reactivity of reduced, native Cp20 toward DTNB suggests that the two detectable thiols are quite accessible in the native enzyme. Previous work has shown that *S. typhimurium* AhpC contains an intersubunit disulfide bond (Cys46–Cys165', two per dimer) that is responsible for the enzyme's peroxidase and DTNB reductase activities (35). Based on sequence alignments, Cys50 and Cys167 of Cp20 are the functional equivalents of Cys46 and Cys165 in *S. typhimurium* AhpC. Cp20 has a third cysteine residue (Cys76), which is not conserved in *S. typhimurium* AhpC or other 2-Cys Prxs. It can thus be predicted that Cys50 and Cys167 account for the reactivity of reduced, native Cp20 toward DTNB and that Cys76 is buried in the native enzyme and plays no role in the catalytic mechanism of the protein. Cp20, like AhpC, is therefore expected to have two active site disulfide centers per dimer with the two subunits in a head-to-tail configuration (35).

*Multiple Sequence Alignment of Cp34, TrxR, and AhpF.* As indicated by the structural and functional properties described herein, Cp34 is a member of the subfamily of flavoprotein reductases including bacterial TrxR and AhpF, yet represents a third branch within this group with properties

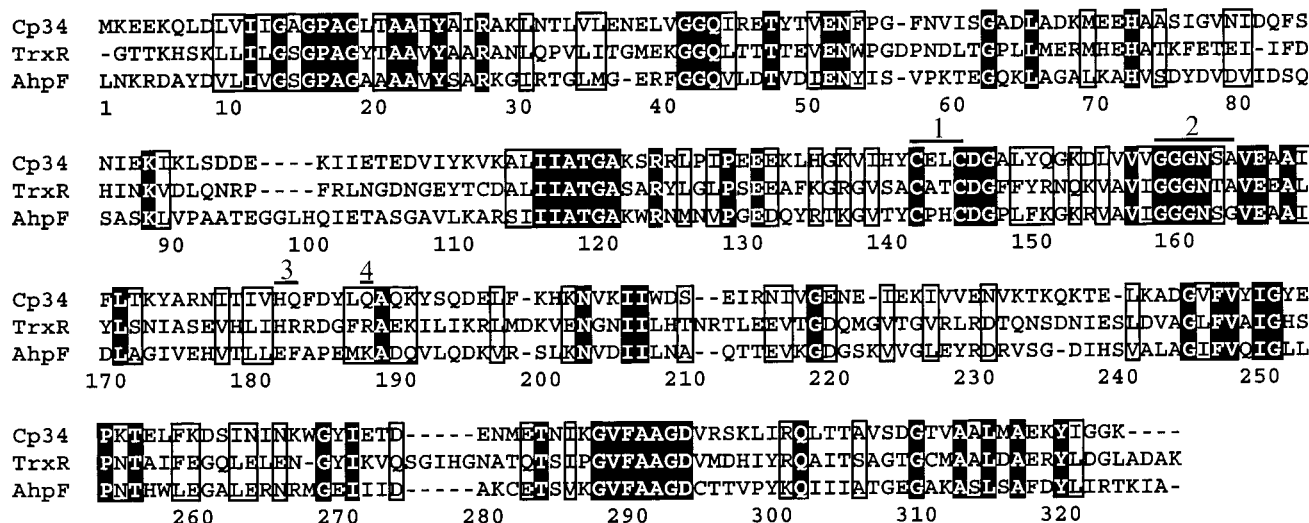


FIGURE 3: Alignment of the amino acid sequences of *C. pasteurianum* Cp34, *E. coli* TrxR, and *S. typhimurium* AhpF. Identical residues at the same position in all the aligned sequences are in black boxes. Positions with similar amino acids are denoted by white boxes. Specific amino acid regions within the alignment are as follows: Region 1, conserved redox-active disulfide centers; Region 2, GxGxx/a motif involved in pyridine nucleotide binding; Regions 3 and 4, residues which are thought to confer specificity for either NADPH (TrxR) or NADH (Cp34 and AhpF). Residues imparting specificity toward NADPH for TrxR include His175 and Arg176 of Region 3 and Arg181 of Region 4. Similarly, Glu385 of AhpF (Region 3) promotes the selectivity of that protein for NADH over NADPH. Cp34 shows little conservation among any of these signature residues, but exhibits high specificity for NADH in biochemical studies.

distinct from those of the other two prototypic members. The aligned amino acid sequences of Cp34, TrxR, and AhpF (residues 207–521) are shown in Figure 3. All three flavoproteins contain a redox-active disulfide center (Region 1) within the pyridine nucleotide binding domain. The amino acid sequences of both Cp34 and TrxR contain the structural motif Gly-X-Gly-X-X-Ala (Region 2) common to many NADPH-dependent enzymes (41) while the AhpF sequence has a Gly-X-Gly-X-X-Gly motif, as is usually indicative of specificity for NADH (42). The crystal structure of TrxR (with NADP<sup>+</sup> bound) also revealed other residues that help stabilize TrxR's interaction with NADP<sup>+</sup> (34) (Regions 3 and 4 in Figure 3). Region 3 of Figure 3 highlights two TrxR residues, His175 and Arg176, that interact with the 2'-phosphate of the adenine base of NADP<sup>+</sup>. A second arginine (Arg181) (Region 4) interacts with the pyrophosphate and the adenine ribose. His175 is conserved within Cp34 but not AhpF, and both arginine residues of TrxR (Arg176 and Arg181) have been replaced by glutamine residues in Cp34. Though Cp34 does have the Gly-X-Gly-X-X-Ala motif common to many NADPH-utilizing enzymes, the replacement of the two critical arginine residues by Gln177 and Gln182 must deter NADPH binding and favor NADH binding because Cp34, like AhpF, exhibits a high specificity for NADH (vide infra).

**Properties of the Bound Flavin of Cp34, TrxR, and AhpF.** ESI-MS analysis of the flavin released from denatured Cp34 revealed FAD as the noncovalently bound cofactor. Treatment of the Cp34-derived flavin with *N. naja* venom phosphodiesterase also resulted in an approximately 10-fold increase in flavin fluorescence indicative of the conversion of FAD to FMN by the phosphodiesterase (43). The fluorescence of the bound FAD of Cp34 was compared to that of the bound FAD of TrxR and AhpF and to free FMN (Table 2). Surprisingly, the FAD fluorescence of Cp34 ( $\lambda_{\max, \text{ex}} = 450 \text{ nm}$ ,  $\lambda_{\max, \text{em}} = 520 \text{ nm}$ ) is greater than half of the fluorescence observed with free FMN ( $\lambda_{\max, \text{ex}} = 450 \text{ nm}$ ,  $\lambda_{\max, \text{em}} = 525 \text{ nm}$ ) and much greater than that of free FAD

Table 2: Comparison of Properties among Three Low- $M_r$  TrxR Family Members

	Cp34	TrxR	AhpF
no. of amino acids	308	320	521
bound FAD fluorescence relative to free FMN (%)	55.6	12.6	4.1
extinction coefficient of bound FAD ( $\text{mM}^{-1} \text{cm}^{-1}$ )	12.7	11.3	13.1
flavin absorbance maxima (nm)	384 & 450	380 & 455	380 & 450
maximal semiquinone formation during dithionite titrations (%)	90	20–82 <sup>a</sup>	90
amount of dithionite required for complete reduction (equiv/FAD)	~2	~2	~3
pyridine nucleotide preference	NADH	NADPH	NADH
breakpoint in $A_{\sim 350}$ changes during NAD(P)H titrations	1.3	1.6	2.6
disulfide reductase activity with various substrates			
DTNB (direct) <sup>b</sup>	–	–	+
Cp9	+ <sup>c</sup>	+ <sup>d</sup>	–
Trx	–	+	–
transhydrogenase activity <sup>e</sup>	115 ± 10	1340 ± 120	1820 ± 210
oxidase activity <sup>f</sup>	64.7 ± 5.9	<5	84.8 ± 14.0

<sup>a</sup> Semiquinone stabilization is substantially higher in the presence of light and/or EDTA (48); in contrast, no such light or EDTA effect was observed for Cp34 or AhpF. Extent of semiquinone formation was based on an extinction coefficient of  $4790 \text{ M}^{-1} \text{cm}^{-1}$  at 580 nm for this species (5). <sup>b</sup> The inherent DTNB reductase activity of Cp34 and TrxR is very low [ $<25 \mu\text{mol}$  of DTNB reduced  $\text{min}^{-1}$  ( $\mu\text{mol}$  of FAD)<sup>-1</sup>] relative to that of AhpF [ $1500 \mu\text{mol}$  of DTNB reduced  $\text{min}^{-1}$  ( $\mu\text{mol}$  of FAD)<sup>-1</sup>]. <sup>c</sup> Interaction is saturable; see Results for details. <sup>d</sup> Interaction is apparently nonsaturable. <sup>e</sup> Activity is expressed as  $\mu\text{mol}$  of AcPyAD(P)H formed  $\text{min}^{-1}$  ( $\mu\text{mol}$  of bound FAD)<sup>-1</sup>. <sup>f</sup> Activity is expressed as  $\mu\text{mol}$  of NAD(P)H oxidized  $\text{min}^{-1}$  ( $\mu\text{mol}$  of bound FAD)<sup>-1</sup>.

(by 4.9-fold). Generally, the fluorescence of FAD is quenched to a much greater extent than it is in Cp34 due to interaction with the protein environment of the enzyme or, in free FAD, to the stacking interaction with the adenine ring (44–46). As shown in Table 2, the flavin of Cp34 is approximately

4.4-fold more fluorescent than the bound FAD of TrxR ( $\lambda_{\text{max, ex}} = 454 \text{ nm}$ ,  $\lambda_{\text{max, em}} = 517 \text{ nm}$ ), and 13.6-fold more fluorescent than that of AhpF ( $\lambda_{\text{max, ex}} = 450 \text{ nm}$ ,  $\lambda_{\text{max, em}} = 517 \text{ nm}$ ). This observation suggests that FAD has a different protein environment in Cp34 than in TrxR or AhpF.

The visible absorbance spectra for the oxidized flavin groups of Cp34, TrxR, and AhpF are quite similar, although the  $\lambda_{\text{max}}$  values of the flavin peaks are slightly different (Table 2). In addition to their spectral properties, two flavin-mediated catalytic features, oxidase activity and transhydrogenase activity, were compared for AhpF, TrxR, and Cp34 proteins. As shown in Table 2, Cp34 exhibits oxidase activity similar to that measured for AhpF, while TrxR is essentially devoid of this activity. Surprisingly, Cp34 does not exhibit significant transhydrogenase activity like the other two flavoproteins (Table 2). Cp34's low transhydrogenase activity may be a result of structural features, not present in TrxR or AhpF, which hinder AcPyAD<sup>+</sup> binding.

**Anaerobic Reductive Titrations of Cp34.** Dithionite and NADH titrations of Cp34 were conducted to characterize spectral properties of various redox forms and compare these properties with those previously reported for TrxR and AhpF (5, 47). Like TrxR and AhpF, Cp34 does not exhibit a detectable charge-transfer interaction between a nascent thiolate and oxidized FAD. Addition of NADH or dithionite leads to spectral changes indicative of the progressive reduction of FAD and the formation of the blue, neutral semiquinone form of the flavin with absorbance centered around 580 nm (Figure 4 and Figure S1 in Supporting Information). The blue, neutral semiquinone form of the flavin of Cp34 is highly stabilized (~90%) during dithionite and NADH titrations (like AhpF) (5), but is not sensitive to the presence of light and/or EDTA (unlike TrxR) (48). Full reduction of Cp34 requires approximately 2 equiv of dithionite per FAD, further confirming the presence of the disulfide center in addition to the bound FAD. NADH titrations proceed in a similar manner (Figure S1 in Supporting Information), but do not result in complete reduction of the flavin due to the relatively low redox potential of the flavin semiquinone. The low extinction, long  $\lambda$  charge-transfer band centered around 755 nm, present in NADH but not dithionite titrations, is the hallmark of electronic interaction between FADH<sub>2</sub> and NAD(P)<sup>+</sup> in these proteins and may be characteristic of a redox species important in catalysis (5, 49).

**Kinetic Characterization of Cp34 and Substrate Specificities for All Three Flavoproteins.** Cp34 and Cp9 form a general disulfide reductase system capable of rapidly reducing both small-molecule (DTNB) and protein (bovine pancreas insulin) disulfide-containing substrates in the presence of NADH. The kinetic parameters for Cp34's interaction with Cp9 and NADH were determined using a DTNB-linked assay carried out on the stopped-flow spectrophotometer. Like TrxR (27) and AhpF (6), Cp34 exhibits a substituted (ping-pong) mechanism as indicated by lines that intersect on the y-axis in the primary Hanes–Woolf plots (Figure 5) (28). A secondary plot (slope replot) of the data (Figure 5, inset of panel A) yielded the  $K_m^{\text{NADH}}$  and  $k_{\text{cat}}$  values for Cp34 (2.65  $\mu\text{M}$  and 13.9  $\text{s}^{-1}$ , respectively). The  $K_m^{\text{Cp9}}$  value for Cp34, 0.29  $\mu\text{M}$ , was determined from the same type of kinetic analysis of the data (Figure 5, panel B). The catalytic efficiencies,  $k_{\text{cat}}/K_m$ , are  $5.2 \times 10^6$  and  $4.8 \times 10^7 \text{ M}^{-1} \text{ s}^{-1}$

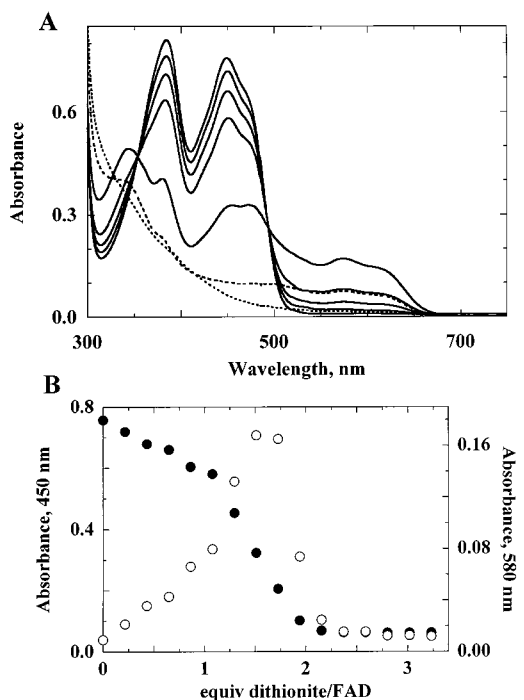


FIGURE 4: Anaerobic dithionite titration of Cp34. The titration was carried out in 25 mM potassium phosphate buffer at pH 7.0 in a total volume of 600  $\mu\text{L}$  at 25  $^{\circ}\text{C}$ . Cp34 (35.7 nmol) was titrated in the presence of 0.36 nmol of methyl viologen with a 5.85 mM solution of dithionite. Spectra were recorded after each addition when no further absorbance changes occurred. Solid lines in panel A represent spectra obtained after the addition of 0, 0.21, 0.64, 1.06, and 1.48 equiv of dithionite/FAD in order of decreasing  $A_{450}$  and increasing  $A_{580}$ . Dashed lines indicate spectra obtained after the addition of 1.91 and 2.33 equiv of dithionite/FAD in order of decreasing  $A_{450}$  and decreasing  $A_{580}$ . Panel B shows the absorbance changes at 450 (closed circles) and 580 nm (open circles) versus equiv of dithionite/FAD added.

for the interaction of Cp34 with NADH and Cp9, respectively. These second-order rate constants are similar to values previously determined for TrxR and AhpF interactions with NAD(P)H and their respective substrate proteins, Trx and AhpC (6, 18, 50).

Although Cp34 does exhibit some ability to utilize NADPH in the DTNB-linked assay with Cp9, the  $K_m^{\text{NADPH}}$  was too high to measure accurately; the Cp34–NADPH interaction does not saturate with concentrations of NADPH as high as 300  $\mu\text{M}$ . However, the second-order rate constant for the Cp34–NADPH interaction, in the presence of 15  $\mu\text{M}$  Cp9, is  $5.0 \times 10^4 \text{ M}^{-1} \text{ s}^{-1}$ , a catalytic efficiency around 100-fold lower than that determined for the Cp34–NADH interaction.

The ability of Cp34 to reduce *E. coli* Trx or for TrxR to reduce Cp9 was determined using the DTNB-linked assay. The reduction of Cp9 by *E. coli* TrxR was linearly dependent on the concentration of Cp9, indicating a simple bimolecular, nonsaturable interaction with a second-order rate constant of  $1.1 \times 10^5 \text{ M}^{-1} \text{ s}^{-1}$ . Cp34 was incapable of reducing *E. coli* Trx over the range of concentrations tested, indicating that Cp34 has a relatively narrow specificity range that includes Cp9 but not Trx-like proteins.

The *E. coli* TrxR–Trx system has previously been shown to efficiently reduce the interchain disulfide bonds of insulin (29). The Cp34–Cp9 system also possesses the ability to reduce insulin. The kinetic parameters determined for Cp34

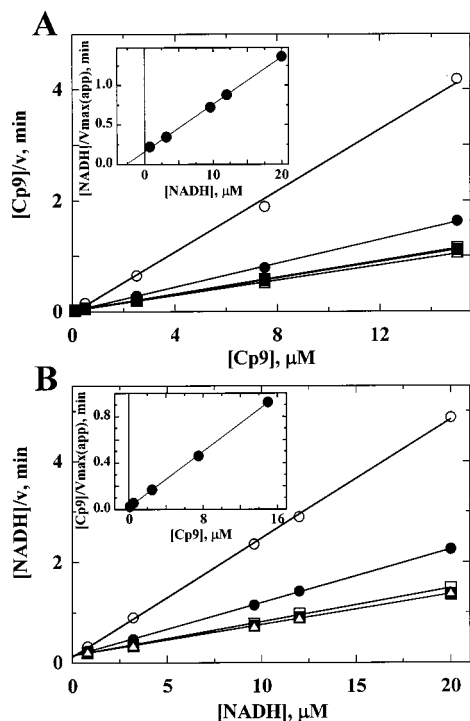


FIGURE 5: Steady-state kinetic analysis of Cp34. Panel A: Hanes–Woolf plot of  $[\text{Cp9}]/v$  versus  $[\text{Cp9}]$  varied at different NADH concentrations. Initial rate data are shown for  $0.8 \mu\text{M}$  (open circles),  $3.2 \mu\text{M}$  (closed circles),  $9.6 \mu\text{M}$  (open squares),  $12 \mu\text{M}$  (closed squares), and  $20 \mu\text{M}$  (open triangles). Inset: Secondary plot of the primary plot versus  $[\text{NADH}]$  to obtain  $k_{\text{cat}}$  and  $K_{\text{m}}^{\text{NADH}}$ . Panel B: Hanes–Woolf plot of  $[\text{NADH}]/v$  versus  $[\text{NADH}]$  varied at different Cp9 concentrations. Initial rate data are shown for  $0.1 \mu\text{M}$  (open circles),  $0.5 \mu\text{M}$  (closed circles),  $2.5 \mu\text{M}$  (open squares),  $7.5 \mu\text{M}$  (closed squares), and  $15 \mu\text{M}$  (open triangles). Inset: Secondary plot of the slopes of the primary plot versus  $[\text{Cp9}]$  to obtain  $k_{\text{cat}}$  and  $K_{\text{m}}^{\text{Cp9}}$ .

using the insulin-reduction assays were comparable to the true  $k_{\text{cat}}$  and true  $K_{\text{m}}$  values determined using the DTNB-linked assay (vide supra) [ $16.1 \pm 1.4 \text{ s}^{-1}$  and  $2.68 \pm 0.83 \mu\text{M}$  for the  $k_{\text{cat}}(\text{app})$  and  $K_{\text{m}}^{\text{Cp9}}(\text{app})$ , respectively, of Cp34]. Cp34 and Cp9 appear to be a general disulfide reductase system with the capacity to reduce various disulfide-containing molecules much like the *E. coli* TrxR–Trx system. The insulin-linked assay was also used to assess AhpF's ability to reduce Cp9. AhpF was previously shown to lack the ability to reduce Trx in the insulin-linked assay (18), and, similarly, AhpF could not reduce Cp9 in the assay.

The proximity of *cp34/cp9* to *rub* in the genome of *C. pasteurianum* also prompted us to determine whether the Cp34–Cp9 system could serve as a reductase for rubredoxin. The ability of the Cp34–Cp9 system to reduce *C. pasteurianum* rubredoxin was assessed by monitoring the associated decrease in  $A_{490}$  as rubredoxin becomes reduced. Although we were able to demonstrate rapid reduction of rubredoxin by spinach Fd-NADP<sup>+</sup> reductase, neither Cp34 nor Cp9 was able to act as a direct reductant of rubredoxin. This result was in agreement with a previous study which indicated that rubredoxin reduction in *C. pasteurianum* is strictly NADPH-dependent (51).

**Peroxidase Assays with Cp34, Cp9, and Cp20.** Cp34, Cp9, and Cp20 form an alkyl hydroperoxide reductase system capable of reducing cumene hydroperoxide,  $\text{H}_2\text{O}_2$ , and ethyl hydroperoxide (Figure 6). All three protein components are

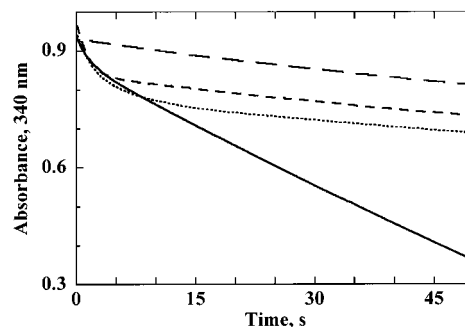


FIGURE 6: Peroxidase assays with Cp34, Cp9, and Cp20. NADH oxidation was monitored at 340 nm on a stopped-flow spectrofluorometer for assay mixtures containing Cp34 ( $0.5 \mu\text{M}$ ), Cp9 ( $10 \mu\text{M}$ ), and Cp20 ( $10 \mu\text{M}$ ) in the absence of hydroperoxide substrate (dotted line) or in the presence of  $1 \text{ mM}$  cumene hydroperoxide (solid line). Assays were also conducted in the presence of  $1 \text{ mM}$  cumene hydroperoxide where Cp20 (short-dashed line) or Cp9 (long-dashed line) was omitted from the assay mixture. Other assays (not shown) with Cp34, Cp9, and Cp20, where  $\text{H}_2\text{O}_2$  or ethyl hydroperoxide was substituted for cumene hydroperoxide, exhibited the same rate of NADH oxidation that was observed with cumene hydroperoxide.

necessary in order to achieve the sustained loss of  $A_{340}$  as NADH is consumed and the hydroperoxide is converted to the corresponding alcohol and water. When either Cp20 or the hydroperoxide substrate is omitted from the assay mixture, the decrease in  $A_{340}$  is observed as a burst, followed by a much lower rate ( $0.42 \mu\text{M}$  NADH oxidized  $\text{s}^{-1}$  versus  $1.70 \mu\text{M}$  NADH oxidized  $\text{s}^{-1}$  when all three proteins are present in the assay); the burst of NADH oxidation can be attributed to the reduction of the protein components present in that particular assay. The low rate of NADH oxidation observed in the absence of Cp9, Cp20, or the hydroperoxide substrate can be attributed to the oxidase activity of Cp34 (see Table 2). Peroxidase assays in which AhpF was substituted for both Cp34 and Cp9 (not shown) did not exhibit a sustained loss of  $A_{340}$ , in contrast to the assays with Cp34, Cp9, and Cp20. Much like the Prx from *H. pylori* (7), the Prx from *C. pasteurianum*, Cp20, appears to be unable to receive electrons from AhpF. It appears that 2-Cys Prxs from bacteria that do not express an AhpF, like *C. pasteurianum* and *H. pylori*, can only receive electrons from low- $M_r$  redox mediators such as Cp9 or Trx. The structural attributes of these 2-Cys Prxs which forbid their reduction by AhpF are not readily apparent, but clearly certain features of AhpC that allow its reactivation by AhpF must be absent from the Prxs from *C. pasteurianum* and *H. pylori*.

**Fluorometric Assay of Cp20 Reduction by DTT-Reduced Cp9.** Previous studies have revealed that the two redox forms of *E. coli* Trx (i.e., reduced or oxidized) have different tryptophan fluorescence spectra, with the reduced form of Trx exhibiting approximately 3-fold higher tryptophan fluorescence (52, 53). Much like Trx, Cp9 also exhibits an increase (by  $\sim 2$ -fold) in tryptophan fluorescence when the protein is converted from its oxidized to its reduced form. It was therefore possible to utilize this difference to characterize the interaction between reduced Cp9 and Cp20 during turnover with  $\text{H}_2\text{O}_2$ . As shown in Figure 7, the amount of Cp9 oxidized per second was linear with respect to the amount of Cp9 in the assay, indicating that the interaction between Cp9 and Cp20 is nonsaturable up to  $35 \mu\text{M}$  Cp9. The second-order rate constant,  $5.2 \times 10^3 \text{ M}^{-1} \text{ s}^{-1}$ , for the

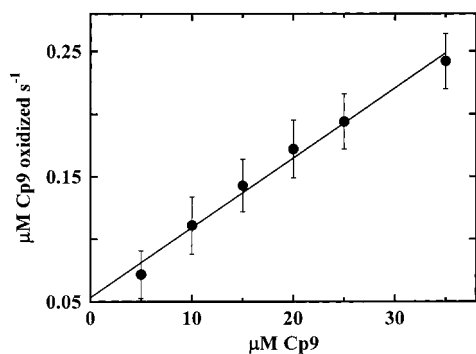


FIGURE 7: Fluorometric peroxidase assays with Cp9 and Cp20. Reduced Cp9, 5–35  $\mu\text{M}$ , in one syringe was mixed with Cp20 (1  $\mu\text{M}$ ) and  $\text{H}_2\text{O}_2$  (1 mM) in the other syringe (all given as final concentrations). The decrease in fluorescence was converted to the amount of Cp9 oxidized per second using the formula presented under Experimental Procedures. The activity measured was plotted against the amount of reduced Cp9 present in the assay to determine the second-order rate constant between Cp9 and Cp20.

interaction between Cp9 and Cp20 was determined by linear regression analysis of the data. Similarly, the interaction between *H. pylori* Trx and the *H. pylori* Prx component was also found to be nonsaturable, although this interaction was found to have a higher second-order rate, at  $1.0 \times 10^5 \text{ M}^{-1} \text{ s}^{-1}$  (7).

Because the ESI-MS and N-terminal sequence analyses indicated heterogeneity in the Cp20 preparation, at least at residue 3, we also tested the activity of a different sample of Cp20 which was isolated from bacteria that were not grown in the fermentor. In this case, ESI-MS analysis revealed that only  $\sim 29\%$  of the Cp20 subunits were of the lower molecular weight (compared to  $\sim 55\%$  in the other preparation), and that homodimeric, native enzyme was the predominant species in the oxidized sample. When the latter Cp20 sample was utilized in the fluorometric assay, the Cp9–Cp20 interaction was likewise nonsaturable, and the second-order rate constant was the same as that determined with the more heterogeneous Cp20 preparation. These data strongly suggest that the Arg $\rightarrow$ Lys codon misread(s) do(es) not affect the Cp9–Cp20 interaction. Indeed, this result is reasonable given the predicted large distance between the third residue and the active site cysteines ( $\sim 23 \text{ \AA}$ ) and also the lack of conservation of this Arg residue in the various homologues of Cp20 (3).

**Comparison of Cp34, Cp9, and Cp20 to Other Clostridial Proteins.** To ascertain any relationship between the Cp34 and Cp9 proteins of this study and the previously characterized Fd-TrxR and Trx proteins from *C. pasteurianum* (32, 33), we obtained Fd-TrxR and Trx samples from Dr. Buchanan for  $\text{NH}_2$ -terminal sequence analysis. Edman degradation of the two proteins yielded the following sequences: MEERYDIAIIGSGPAGLSAAINAKIR (Protein Information Resource accession no. A59395) and MVKDIND-SNFQEEVKAGTVVDF (PIR accession no. A59394) for Fd-TrxR and Trx, respectively. The N-terminal sequence data obtained for each of the proteins clearly established that the Fd-dependent TrxR–Trx system is quite distinct from the NADH-dependent Cp34–Cp9 system presented in this report. Thus, *C. pasteurianum* codes for at least two different low- $M_r$  TrxR family members, Cp34 and the Fd-dependent TrxR.

After searching the recently completed genomic database of *Clostridium acetobutylicum* (54) for homologues of the *C. pasteurianum* alkyl hydroperoxide reductase proteins described in this report, it was discovered that the *C. acetobutylicum* genome encodes two different low- $M_r$  TrxR homologues. One of the TrxR-like gene products (orf CAC0869) has 70% identity to Cp34 at the amino acid level, the highest identity to Cp34 of all the low- $M_r$  TrxRs identified to date. The other *C. acetobutylicum* TrxR-like gene product (orf CAC3082) is only distantly related to Cp34 (34% amino acid identity), but has 88% amino acid identity to the N-terminal sequence obtained for the *C. pasteurianum* Fd-TrxR. We therefore predict that this low- $M_r$  TrxR homologue, like the protein from *C. pasteurianum*, is also an Fd-dependent TrxR. The gene for this *fd-trxR* homologue is positioned directly downstream of a gene for a *trx* homologue (orf CAC3083) in the *C. acetobutylicum* genome, suggesting that the two gene products form a Fd-dependent TrxR–Trx system quite similar to the system isolated from *C. pasteurianum* by Buchanan's group (32, 33).

The gene encoding the Cp34-like TrxR homologue is not proximal to genes for *cp9* and *cp20* homologues in the *C. acetobutylicum* genome as is the case for *C. pasteurianum*. A *cp9*-like gene (orf CAC2777) was identified in the *C. acetobutylicum* genome (68% amino acid identity to Cp9), but this gene is  $\sim 1.9 \text{ Mb}$  away from the *cp34*-like gene. Given our findings, it is likely that this Cp9-like protein is a substrate for the Cp34-like protein even though the two genes are not adjacent to one another in the genome. Indeed, the genes for *trxR* and *trx* in most organisms, including *E. coli*, are not positioned proximal to one another in their respective genomes (55). Surprisingly, a homologue of *cp20*, i.e., a 2-Cys Prx, was not identified within the *C. acetobutylicum* genome using BLAST (56), although a gene product that has 39% amino acid identity to *E. coli* "thiol peroxidase" was identified (orf CAC3306).

Our studies have established that the Cp34–Cp9 system can participate in oxidative stress protection in *C. pasteurianum*, while the cellular role of the Fd-dependent TrxR–Trx system remains unclear. It is possible the Fd-dependent system is needed for deoxyribonucleotide synthesis and/or general cell homeostasis, like the *E. coli* TrxR–Trx system (57–59), although we have also provided evidence herein that the Cp34–Cp9 system could provide such a generalized protein disulfide reductase function, as well. We cannot rule out the possibility that the Fd-dependent TrxR/Trx system could also serve as a reductase system for Cp20 in *C. pasteurianum* under anaerobic, or perhaps even aerobic, conditions. That Grxs and Trxs in other organisms, including *E. coli*, have been shown to have somewhat overlapping cellular functions (60) suggests Cp9 and Trx may reduce some of the same disulfide-containing enzymes. However, the amount of reduced Trx available for Cp20 reduction during conditions of oxidative stress would be predicted to be low due to several factors. The capacity to maintain a pool of reduced Fd during times of oxidative stress is expected to be limited due to the  $\text{O}_2$ -sensitive nature of a key metabolic enzyme, pyruvate–Fd oxidoreductase (PFO) (61). PFO catalyzes the reduction of Fd in *C. pasteurianum* (62) and other anaerobes (63, 64) and has been shown to be extremely sensitive to inactivation by  $\text{O}_2$ . The level of PFO activity in *Bacteroides thetaiotaomicron*, an obligate

anaerobe like *C. pasteurianum*, was shown to be reduced to only 3% of the level of activity observed under anaerobic conditions following aeration of the bacterial cultures (61). Similarly, purified PFO from *C. pasteurianum* has been shown to be rapidly inactivated by O<sub>2</sub> (62). In addition, many iron–sulfur cluster containing enzymes, including Fd from *C. pasteurianum* (65, 66), have been shown to undergo oxidative degradation/inactivation upon exposure to O<sub>2</sub> and ROS (67–70). That Cp34 utilizes the reducing power of NADH, and not Fd, to reduce Cp9 and Cp20 may provide an advantage to *C. pasteurianum* during times of oxidative stress.

**Comparison of Cp9 to Other Grx-like Redox Proteins.** Cp9 is the latest addition to a growing list of Grx-like proteins that have been shown to possess Trx-like activities. Jordan et al. showed that the Grx-like *E. coli* NrdH was capable of reducing insulin and was a good substrate for TrxR (71). In addition, NrdH was not reduced by glutathione, unlike “true” Grxs. Like NrdH, Cp9 has been shown to possess Trx-like activities and is a good substrate for the TrxR-like Cp34 as well as for *E. coli* TrxR. Interestingly, *C. pasteurianum* lacks glutathione (72), indicating that reduced glutathione could not be the physiological source of electrons for Cp9. Two other Grx-like proteins from the archaea *Methanobacterium thermoautotrophicum* and *Methanococcus jannaschii*, which like *C. pasteurianum* cannot synthesize glutathione (73), were also shown to possess significant insulin reductase activity in the presence of DTT (74, 75). Database searches with the Cp9 sequence have revealed another Grx-like protein with 50% amino acid sequence identity to Cp9 within the genome of *Thermotoga maritima* (76). On the basis of these sequence similarities, we predict that this protein and also the two archaeal proteins are substrates for low-*M<sub>r</sub>* TrxR homologues within each of these organisms. These Grx-like proteins may comprise a separate division of the Trx/Grx superfamily that have some or all of the activities (DTNB, insulin, and Prx reductase activities) associated with Trxs, but have structural features more similar to Grxs.

**Comparison of the Alkyl Hydroperoxide Reductase Systems of *C. pasteurianum* and *Chromatium gracile*.** The alkyl hydroperoxide reductase system from *C. pasteurianum* shares several features with an alkyl hydroperoxide reductase system from the anaerobe *C. gracile* described in a recent report (19). Both systems employ Grx-like proteins to mediate electron transfer to the Prx component, although the Grx-like protein is actually fused to the Prx protein in the *C. gracile* system; these represent the first two alkyl hydroperoxide reductase systems shown to include Grx homologues. The flavoprotein component of the *C. gracile* system, glutathione amide reductase (GAR), is reminiscent of Cp34, but is more closely related to the glutathione reductase branch of flavoprotein disulfide reductases than to the low-*M<sub>r</sub>* TrxR protein family. GAR and Cp34 both prefer NADH to NADPH, unlike their respective homologues, *E. coli* glutathione reductase and TrxR. Both Cp34 and GAR also reduce atypical substrates, Cp9 and glutathione amide, respectively, and both flavoproteins have been shown to be part of multienzyme systems that protect against oxidative damage.

**Putative Involvement of Cp20 in the Repair of Oxidized Alk-1-enyl Lipids (Plasmalogens).** The phospholipid content of many species of clostridia, including *C. pasteurianum*,

has been shown to include significant amounts of plasmalogens (77). Raetz et al. have previously proposed that plasmalogens may function as scavengers of ROS and that radical-mediated oxidation of plasmalogens could promote the formation of allylic hydroperoxides (78). Members of the 2-Cys Prx family have been shown to catalyze the reduction of a broad range of hydroperoxide substrates, including lipid hydroperoxides (4, 7, 8). The considerable plasmalogen content of *C. pasteurianum*'s phospholipid membrane and the predicted susceptibility of these molecules to oxidative damage suggest that Cp20 may play an extremely important role in the repair of damaged plasma membrane components.

**Summary.** A unique alkyl hydroperoxide reductase system has been identified in the anaerobe *C. pasteurianum*. This system is composed of an unusual NADH-utilizing low-*M<sub>r</sub>* TrxR family member (Cp34), a Grx homologue (Cp9), and a 2-Cys Prx (Cp20). Cp34 and Cp9 form an efficient NADH-dependent system capable of reducing DTNB, insulin, and Cp20. Cp9 is the first example of a Grx-like protein that directly mediates electron transfer from a TrxR-like flavoprotein to a Prx. This unusual alkyl hydroperoxide reductase system is expected to be an important defense against oxidative stress due to the likely absence of catalase in *C. pasteurianum*.

## ACKNOWLEDGMENT

We thank Debra Regier for constructing pOXO4/*cp20*, and Dr. Bob Buchanan at the University of California, Berkeley, for his gift of *C. pasteurianum* Fd-TrxR and Trx. We are also grateful to Laura M. S. Baker for purifying *E. coli* TrxR and Trx.

## SUPPORTING INFORMATION AVAILABLE

A figure of an anaerobic NADH titration of Cp34 (Figure S1) is included as Supporting Information. This material is available free of charge via the Internet at <http://pubs.acs.org>.

## REFERENCES

- Jenney, F. E., Jr., Verhagen, M. F., Cui, X., and Adams, M. W. (1999) *Science* 286, 306–309.
- Lombard, M., Houee-Levin, C., Touati, D., Fontecave, M., and Niviere, V. (2001) *Biochemistry* 40, 5032–5040.
- Chae, H. Z., Robison, K., Poole, L. B., Church, G., Storz, G., and Rhee, S. G. (1994) *Proc. Natl. Acad. Sci. U.S.A.* 91, 7017–7021.
- Jacobson, F. S., Morgan, R. W., Christman, M. F., and Ames, B. N. (1989) *J. Biol. Chem.* 264, 1488–1496.
- Poole, L. B. (1996) *Biochemistry* 35, 65–75.
- Poole, L. B., and Ellis, H. R. (1996) *Biochemistry* 35, 56–64.
- Baker, L. M. S., Raudonikiene, A., Hoffman, P. S., and Poole, L. B. (2001) *J. Bacteriol.* 183, 1961–1973.
- Nogoceke, E., Gommel, D. U., Kiess, M., Kalisz, H. M., and Flohé, L. (1997) *J. Biol. Chem.* 378, 827–836.
- Poole, L. B., Reynolds, C. M., Wood, Z. A., Karplus, P. A., Ellis, H. R., and Li Calzi, M. (2000) *Eur. J. Biochem.* 267, 6126–6133.
- Chae, H. Z., Chung, S. J., and Rhee, S. G. (1994) *J. Biol. Chem.* 269, 27670–27678.
- Singleton, P., and Sainsby, D. (1987) *Dictionary of microbiology and molecular biology*, 2nd ed., John Wiley and Sons Ltd., New York.
- Mathieu, I., Meyer, J., and Moulis, J. M. (1992) *Biochem. J.* 285, 255–262.

13. Altschul, S. F., Madden, T. L., Schaffer, A. A., Zhang, J., Zhang, Z., Miller, W., and Lipman, D. J. (1997) *Nucleic Acids Res.* 25, 3389–3402.
14. Thompson, J. D., Higgins, D. G., and Gibson, T. J. (1994) *Nucleic Acids Res.* 22, 4673–4680.
15. Parsonage, D., Miller, H., Ross, R. P., and Claiborne, A. (1993) *J. Biol. Chem.* 268, 3161–3167.
16. Ausubel, F. M., Brent, R. B., Kingston, R. E., Moore, D. D., Seidman, J. G., Smith, J. A., and Struhl, K. E. (1999) *Short protocols in molecular biology*, John Wiley & Sons, Inc., New York.
17. Poole, L. B., Godzik, A., Nayeem, A., and Schmitt, J. D. (2000) *Biochemistry* 39, 6602–6615.
18. Reynolds, C. M., and Poole, L. B. (2000) *Biochemistry* 39, 8859–8869.
19. Vergauwen, B., Pauwels, F., Jacquemotte, F., Meyer, T. E., Cusanovich, M. A., Bartsch, R. G., and Van Beeumen, J. J. (2001) *J. Biol. Chem.* 276, 20890–20897.
20. Johnson, M., Correia, J. J., Yphantis, D. A., and Halvorson, H. (1981) *Biophys. J.* 36, 575–588.
21. Laue, T. M., Shah, B. D., Ridgeway, T. M., and Pelletier, S. L. (1992) in *Analytical ultracentrifugation in biochemistry and polymer science* (Harding, S. E., Rowe, A. J., and Horton, J. C., Eds.) pp 90–125, The Royal Society of Chemistry, Cambridge.
22. Williams, C. H., Jr., Zanetti, G., Arscott, L. D., and McAllister, J. K. (1967) *J. Biol. Chem.* 242, 5226–5231.
23. Holmgren, A., and Reichard, P. (1967) *Eur. J. Biochem.* 2, 187–196.
24. Kümmerle, R., Zhuang-Jackson, H., Gaillard, J., and Moulis, J. M. (1997) *Biochemistry* 36, 15983–15991.
25. Shin, M. (1971) *Methods Enzymol.* 23, 440–447.
26. Batie, C. J., LaHaie, E., and Ballou, D. P. (1987) *J. Biol. Chem.* 262, 1510–1518.
27. Prongay, A. J., Engelke, D. R., and Williams, C. H., Jr. (1989) *J. Biol. Chem.* 264, 2656–2664.
28. Cornish-Bowden, A. (1999) *Fundamentals of enzyme kinetics*, Portland Press, Ltd., London.
29. Holmgren, A. (1984) *Methods Enzymol.* 107, 295–300.
30. Leatherbarrow, R. (1987) ENZFITTER, Biosoft, Cambridge, U.K.
31. Peterson, J. A., Kusunose, M., Kusunose, E., and Coon, M. J. (1967) *J. Biol. Chem.* 242, 4334–4340.
32. Hammel, K. E., and Buchanan, B. B. (1981) *FEBS Lett.* 130, 88–92.
33. Hammel, K. E., Cornwell, K. L., and Buchanan, B. B. (1983) *Proc. Natl. Acad. Sci. U.S.A.* 80, 3681–3685.
34. Waksman, G., Krishna, T. S. R., Williams, C. H., Jr., and Kuriyan, J. (1994) *J. Mol. Biol.* 236, 800–816.
35. Ellis, H. R., and Poole, L. B. (1997) *Biochemistry* 36, 13349–13356.
36. Rosenberg, A. H., Goldman, E., Dunn, J. J., Studier, F. W., and Zubay, G. (1993) *J. Bacteriol.* 175, 716–722.
37. Kane, J. F. (1995) *Curr. Opin. Biotechnol.* 6, 494–500.
38. Hirotsu, S., Abe, Y., Okada, K., Nagahara, N., Hori, H., Nishino, T., and Hakoshima, T. (1999) *Proc. Natl. Acad. Sci. U.S.A.* 96, 12333–12338.
39. Alphey, M. S., Bond, C. S., Tetaud, E., Fairlamb, A. H., and Hunter, W. N. (2000) *J. Mol. Biol.* 300, 903–916.
40. Schröder, E., Littlechild, J. A., Lebedev, A. A., Errington, N., Vagin, A. A., and Isupov, M. N. (2000) *Struct. Fold. Des.* 8, 605–615.
41. Hanukoglu, I., and Gutfinger, T. (1989) *Eur. J. Biochem.* 180, 479–484.
42. Scrutton, N. S., Berry, A., and Perham, R. N. (1990) *Nature* 343, 38–43.
43. Bessey, O. A., Lowry, O. H., and Love, R. H. (1949) *J. Biol. Chem.*, 755–769.
44. Song, P. S. (1971) in *Flavins and Flavoproteins* (Kamin, H., Ed.) pp 37–61, University Park Press, Baltimore, MD.
45. Sun, M., Moore, T. A., and Song, P. S. (1972) *J. Am. Chem. Soc.* 94, 1730–1740.
46. Ghisla, S., Massey, V., Lhoste, J. M., and Mayhew, S. G. (1974) *Biochemistry* 13, 589–597.
47. Zanetti, G., and Williams, C. H., Jr. (1967) *J. Biol. Chem.* 242, 5232–5236.
48. Zanetti, G., Williams, C. H., Jr., and Massey, V. (1968) *J. Biol. Chem.* 243, 4013–4019.
49. Lennon, B. W., and Williams, C. H., Jr. (1996) *Biochemistry* 35, 4704–4712.
50. Lennon, B. W., and Williams, C. H., Jr. (1997) *Biochemistry* 36, 9464–9477.
51. Lovenberg, W. (1972) *Methods Enzymol.* 24, 477–480.
52. Stryer, L., Holmgren, A., and Reichard, P. (1967) *Biochemistry* 6, 1016–1020.
53. Holmgren, A. (1972) *J. Biol. Chem.* 247, 1992–1998.
54. Nölling, J., Breton, G., Omelchenko, M. V., Makarova, K. S., Zeng, Q., Gibson, R., Lee, H. M., Dubois, J., Qiu, D., Hitti, J., Wolf, Y. I., Tatusov, R. L., Sabathe, F., Doucette-Stamm, L., Soucaille, P., Daly, M. J., Bennett, G. N., Koonin, E. V., and Smith, D. R. (2001) *J. Bacteriol.* 183, 4823–4838.
55. Kreimer, S., Sohling, B., and Andreesen, J. R. (1997) *Arch. Microbiol.* 168, 328–337.
56. Altschul, S. F., Gish, W., Miller, W., Myers, E. W., and Lipman, D. J. (1990) *J. Mol. Biol.* 215, 403–410.
57. Holmgren, A. (1989) *J. Biol. Chem.* 264, 13963–13966.
58. Prinz, W. A., Ålund, F., Holmgren, A., and Beckwith, J. (1997) *J. Biol. Chem.* 272, 15661–15667.
59. Williams, C. H., Jr. (1995) *FASEB J.* 9, 1267–1276.
60. Åslund, F., and Beckwith, J. (1999) *J. Bacteriol.* 181, 1375–1379.
61. Pan, N., and Imlay, J. A. (2001) *Mol. Microbiol.* 39, 1562–1571.
62. Moulis, J.-M., Davasse, V., Meyer, J., and Gaillard, J. (1996) *FEBS Lett.* 380, 287–290.
63. Pieulle, L., Guigliarelli, B., Asso, M., Dole, F., Bernadac, A., and Hatchikian, E. C. (1995) *Biochim. Biophys. Acta* 1250, 49–59.
64. Kunow, J., Linder, D., and Thauer, R. K. (1995) *Arch. Microbiol.* 163, 21–28.
65. Bertini, I., Briganti, F., Calzolari, L., Messori, L., and Scozzafava, A. (1993) *FEBS Lett.* 332, 268–272.
66. Camba, R., and Armstrong, F. A. (2000) *Biochemistry* 39, 10587–10598.
67. Khoroshilova, N., Popescu, C., Munck, E., Beinert, H., and Kiley, P. J. (1997) *Proc. Natl. Acad. Sci. U.S.A.* 94, 6087–6092.
68. Beinert, H., Holm, R. H., and Munck, E. (1997) *Science* 277, 653–659.
69. Ding, H., and Demple, B. (1998) *Biochemistry* 37, 17280–17286.
70. Duin, E. C., Lafferty, M. E., Crouse, B. R., Allen, R. M., Sanyal, I., Flint, D. H., and Johnson, M. K. (1997) *Biochemistry* 36, 11811–11820.
71. Jordan, A., Åslund, F., Pontis, E., Reichard, P., and Holmgren, A. (1997) *J. Biol. Chem.* 272, 18044–18050.
72. Fahey, R. C., Brown, W. C., Adams, W. B., and Worsham, M. B. (1978) *J. Bacteriol.* 133, 1126–1129.
73. Fahey, R. C. (2001) *Annu. Rev. Microbiol.* 55, 333–356.
74. McFarlan, S. C., Terrell, C. A., and Hogenkamp, H. P. (1992) *J. Biol. Chem.* 267, 10561–10569.
75. Lee, D. Y., Ahn, B. Y., and Kim, K. S. (2000) *Biochemistry* 39, 6652–6659.
76. Nelson, K. E., Clayton, R. A., Gill, S. R., Gwinn, M. L., Dodson, R. J., Haft, D. H., Hickey, E. K., Peterson, J. D., Nelson, W. C., Ketchum, K. A., McDonald, L., Utterback, T. R., Malek, J. A., Linher, K. D., Garrett, M. M., Stewart, A. M., Cotton, M. D., Pratt, M. S., Phillips, C. A., Richardson, D., Heidelberg, J., Sutton, G. G., Fleischmann, R. D., Eisen, J. A., Fraser, C. M., et al. (1999) *Nature* 399, 323–329.
77. Johnston, N. C., and Goldfine, H. (1983) *J. Gen. Microbiol.* 129, 1075–1081.
78. Morand, O. H., Zoeller, R. A., and Raetz, C. R. (1988) *J. Biol. Chem.* 263, 11597–11606.